J. Microbiol. Biotechnol. (2009), **19**(3), 299–306
doi: 10.4014/jmb.0801.073
First published online 23 October 2008

JOURNAL OF MICROBIOLOGY AND BIOTECHNOLOGY

Mechanism Analysis of Effect of Oxygen on Molecular Weight of Hyaluronic Acid Produced by *Streptococcus zooepidemicus*

Duan, Xu-Jie, Hong-Xing Niu, Wen-Song Tan, and Xu Zhang*

State Key Laboratory of Bioreactor Engineering, East China University of Science and Technology, Shanghai 200237, P.R.China

Received: January 28, 2008 / Accepted: July 16, 2008

Dissolved oxygen (DO) has a significant effect on the molecular weight of hyaluronic acid (HA) during the fermentation of *Streptococcus zooepidemicus*. Therefore, to further investigate the effect of DO on the yield and molecular weight of HA, this study compared the metabolic flux distribution of *S. zooepidemicus* under aerobic conditions at various DO levels. The metabolic flux analysis demonstrated that the HA synthesis pathway, considered a dependent network, was little affected by the DO level. In contrast, the fluxes of lactate and acetate were greatly influenced, and more ATP was generated concomitant with acetate at a high DO level. Furthermore, the *has* gene expression and HA synthase activity were both repressed under anaerobic conditions, yet not obviously affected under aerobic conditions at various DO levels. Therefore, it was concluded that the HA molecular weight would seem to depend on the concomitant effect of the generation of ATP and reactive oxygen species. It is expected that this work will contribute to a better understanding of the effect of the DO level on the mechanism of the elongation of HA chains.

Keywords: Oxygen, hyaluronic acid, metabolic flux analysis, hyaluronic acid synthase, reactive oxygen species

Hyaluronic acid (HA) is a linear polysaccharide that consists of two alternating sugars, glucuronic acid and N-acetylglucosamine. HA plays an important role in living organisms owing to its high molecular weight and unique viscoelastic and rheological properties, plus it has a wide variety of applications in biomedicine and industry [13, 18].

Commercially, HA is produced *via* extraction from rooster combs or by the pathogenic Gram-positive bacterium *Streptococcus zooepidemicus* [7]. *S. zooepidemicus*, a facultative anaerobe, can grow under both anaerobic and aerobic conditions, and the effect of the DO level on the yield and molecular weight of HA during HA fermentation has already been extensively discussed by several researchers [1, 6, 11, 12, 15, 16]. Huang *et al*. [12] and Duan *et al*. [6] both found that a higher HA yield was obtained in the case of aerobic cultivation when compared with anaerobic cultivation, and although the DO level had little effect on the HA yield, it had a significant effect on the HA molecular weight. Armstrong and Johns [1] and Kim *et al*. [15] also observed that aeration favored the HA molecular weight, although a high aeration rate or DO level caused a decrease in the HA molecular weight [6, 15]. However, since most previous studies on HA fermentation have focused on optimizing the fermentation parameters, little attention has been paid to the reasons for the variation in the HA molecular weight.

A metabolic flux analysis (MFA) is a powerful methodology for determining metabolic pathway fluxes, and comparing the metabolic flux responses to environmental perturbation can further the current understanding of cellular physiology and metabolism [2, 17, 20]. The metabolism of glucose and maltose during HA fermentation was already compared by Fong Chong and Nielsen [8], and it was found that changing the sugar source had little impact on the HA yield and molecular weight. Meanwhile, Gao *et al*. [10] used an MFA to demonstrate that a low DO concentration favored the HA yield.

In previous work, the current authors found that whereas a high DO level favored the HA molecular weight, the HA molecular weight decreased at a DO level of 80% [6]. However, the detailed metabolic characteristics have not yet been clarified. Therefore, this study attempted to reveal the reasons for the difference in the HA molecular weight according to the DO level using an MFA. Thus, the detailed metabolic flux and key enzyme HA synthase (HAS) in the synthesis of HA were analyzed. Moreover, the generation of reactive oxygen species (ROS) was also determined to elucidate the decrease in the HA molecular weight with a high level of DO. Therefore, the results of this study are

*Corresponding author
Phone: +86-21-64252536; Fax: +86-21-64252250;
E-mail: zhangxu@ecust.edu.cn

expected to further the current understanding of the effect of the DO level on the HA molecular weight during HA fermentation.

Materials and Methods

Bacterial Strain

S. zooepidemicus G1, a mutant of *S. zooepidemicus* ATCC 39920 induced by exposure to ultraviolet (UV) light and *N*-methyl-*N'*-nitro-*N*-nitrosoguanidine, was used in this study.

Cultivation Conditions

The isolation of a pure culture was achieved by streaking onto agar plates that contained in g/l 2 of glucose, 10 of beef extract, 20 of polypeptone, 5 of yeast extract, 2 of NaCl, 1 of Na_2HPO_4, 0.12 of KH_2PO_4, and 20 of agar. The inoculum was prepared in a 250-ml shake flask with 30 ml of a medium that consisted of in g/l 2 of glucose, 10 of beef extract, 20 of polypeptone, 5 of yeast extract, 2 of NaCl, 1 of Na_2HPO_4, and 0.12 of KH_2PO_4, and incubated at 37°C for 8 h.

The fermentation for HA production was carried out in a 5-l fermentor (BIOREA-2000, Shanghai, China) with a working volume of 3-l. The agitation was provided by two six-blade disk turbines and one anchor. The medium composition was as follows (g/l): 20 of polypeptone, 10 of yeast extract, 2 of NaCl, 1 of $MgSO_4 \cdot 7H_2O$, and 2.5 of K_2HPO_4. The fermentor was inoculated with 5% (v/v) inoculum, and operated at 37°C and pH 7.0 (with 5 M NaOH). The DO level was controlled by mixing the inlet air with oxygen or nitrogen, and the impeller speed was increased stepwise from 150 rpm to 600 rpm. The initial concentration of glucose was 40 g/l, and 50% (w/v) glucose was fed at a feed rate of 0.5–1.0 ml/min to maintain a concentration of around 10 g/l.

Metabolite Measurements

The biomass concentration was measured from the optical density (OD) of the broth at 660 nm using a spectrophotometer (model 752N; Shanghai, China), the cell dry weight determined through the linear correlation between the OD and the dry weight, and the glucose concentration determined using the Miller method [21].

The concentrations of formate, lactate, and acetate were determined from 0.22-μm filtered broth samples. The samples were first centrifuged at 10,000 ×*g* for 30 min to remove the biomass, and then chloroform was added to remove the protein. The HPLC system (Waters 1525 Binary Pump with 717Plus Autosampler; U.S.A.) was equipped with a 250 mm×4.6 mm×5 mm LiChrosorb RP-18 column. The mobile phase was 0.03 M KH_2PO_4, pH 2.5 (with H_3PO_4), and the column was maintained at 25°C. The peak elution profile was monitored using a Waters 2487 dual wavelength absorbance detector at 215 nm. The concentration of ethanol was determined by gas chromatography (GC-900C; Shanghai, China), which was equipped with a 30 m×0.53 mm×1 μm capillary column (AT. SE-54; Lanzhou, China) and flame ionization detector. N_2 was used as the carrier gas. The oven, injector, and detector were maintained at 100, 250, and 250°C, respectively.

The HA concentration was determined using the Bitter-Muir method [3], and the molecular weight of the HA was measured using the Laurent *et al.* method [19]. Single-point measurements were performed on diluted samples containing 200 to 500 μg/ml in 0.2 M NaCl at pH 7.0. The Mark-Houwink constants were $k=3.6\times10^{-4}$ and $a=0.78$.

Quantitative Real-Time RT-PCR Analysis of *has* Gene

The cells were harvested during the exponential phase, centrifuged at 12,000 ×*g* for 30 min, and lysed with 5 mg/ml lysozyme for 10 min. The total RNA was extracted using a Trizol reagent (Invitrogen, U.S.A.) according to the manufacturer's instructions. The RT reaction was undertaken with 3 μg of total RNA in 5 μl of RT buffer (250 mM Tris-HCl, pH 8.3, 200 mM KCl, 40 mM $MgCl_2$, 5 mM DTT) (Progema, U.S.A.), 1.5 μg of primer, 4 μl of 2.5 mM dNTP (Takara, Japan), and 30 units of AMV reverse transcriptase (Promega, U.S.A.) in a total volume of 25 ml. The reaction conditions were 42°C for 1 h, followed by 95°C for 5 min. The reverse primers were 5'GAAGA-TAATCACCAGAAAGGCT3' for the *has* gene and 5'CAGCGTCAG-TTACAGACCAGAG3' for the 16S rRNA (house-keeping gene).

The real-time PCR was performed in 25 μl reaction mixture volumes, including 12.5 μl of real-time PCR mix (Toyobo, Japan), 2 μl of RT reaction product, 0.2 μl of each primer, and DEPC water. The reaction was carried out in a Bio-Rad iCycler iQ Real-Time PCR (Bio-Rad, U.S.A.), and the reaction conditions were 94°C for 5 min, 35 cycles at 94°C for 20 s, 60°C for 20 s, and 72°C for 20 s. The real-time PCR primers were 5'GCTTGACCAACTATGCAACTGA3' and 5'GCCTACAAAGAAATCCACCACA3' for the *has* gene, and 5'GGGAGGCAGCAGTAGGGAATCT3' and 5'AACTTCAGACTTA-TCAAACCGC3' for the 16S rRNA.

HAS Assay

The HAS activity was determined according to Yu and Stephanopoulos [29]. The modified method was as follows: 5-ml broth samples were harvested during the exponential growth phase, centrifuged at 10,000 ×*g* for 30 min, and then resuspended in 20 ml of phosphate buffered saline (pH 7.2). The suspension was sonicated on ice with a 300 W impulse every 4 s for 50 min (FS-300; Shanghai, China). The HAS activity was determined in 1 ml of a 0.5-ml cell lysis solution, 0.25 ml of 4 mM UDP-GlcA, 0.25 ml of 4 mM UDP-GlcNAc, 10 μl of 1 M $MgCl_2$, and 10 μl of 0.1 M DTT. The enzymatic reaction was initiated by placing the mixture in a 37°C bath and incubating for 2 h. The reaction was then terminated by a 2 min immersion into 100°C boiling water, cooling to room temperature, and the addition of an equal volume of 0.1% (w/v) SDS. One unit of HAS activity was defined as 1 mg of HA generated per hour per gram of dry cell.

ROS Measurement

The ROS level was measured using 2',7'-dichlorodihydro-fluorescein diacetate (H_2DCF-DA). One ml broth samples (1×10^7 cells) were centrifuged and treated with 5 μl of 10 μM H_2DCF-DA at 37°C for 20 min. The fluorescence intensity was then determined with excitation and emission wavelengths at 488 and 530 nm, respectively.

Results and Discussion

HA Fermentation Kinetics of *S. zooepidemicus* G1

Fig. 1 shows the profiles of the biomass concentration, glucose concentration, HA concentration, and by-product concentrations (*e.g.*, lactate, acetate, and ethanol) during the HA fermentation with a DO level of 10%. The cultivation of HA can be divided into three phases: lag phase (0–1 h), exponential phase (1–10 h), and stationary phase (10–14 h). During

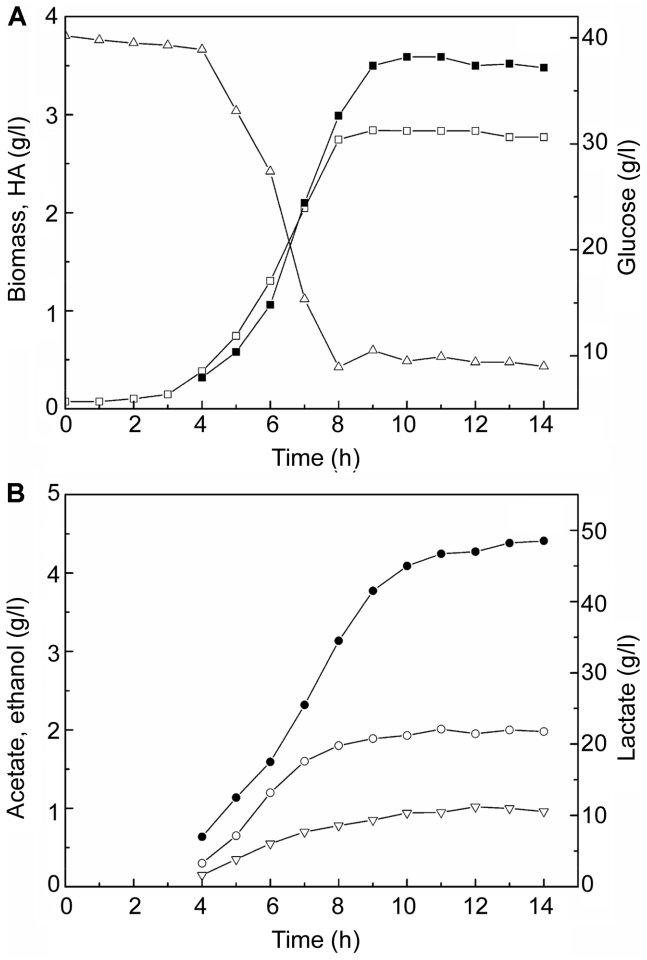

Fig. 1. HA fermentation of *S. zooepidemicus* G1 cultured on complex medium at 10% DO level.
Symbols: (□), biomass; (■), HA; (△), glucose; (○), acetate; (▽), ethanol; (●), lactate.

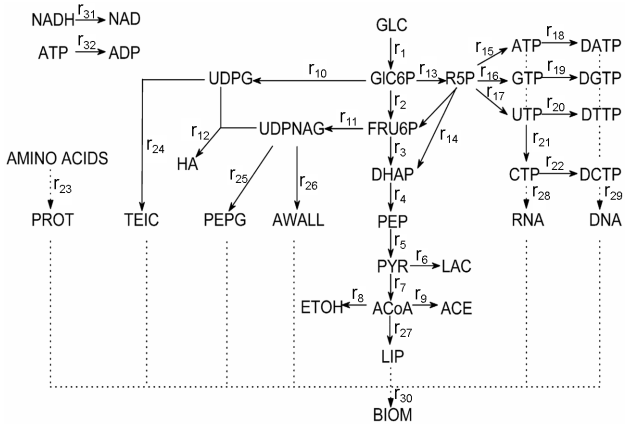

Fig. 2. The metabolic model of *S. zooepidemicus* G1.

Appendix I. The metabolic reactions in *Streptococcus zooepidemicus*.

Reaction No.	Metabolic reactions
r1	GLC+PEP→GLC6P+PYR
r2	GLC6P→FRU6P
r3	FRU6P+ATP→2DHAP+ADP
r4	DHAP+NAD+ADP+PI→PEP+NADH+ATP
r5	PEP+ADP→PYR+ATP
r6	PYR+NADH→LAC+NAD
r7	PYR+CoA+NAD→ACoA+NADH+CO_2
r8	ACoA+2NADH→ETOH+CoA+2NAD
r9	ACoA+ADP+PI→ACE+CoA+ATP
r10	GLC6P+UTP→UDPG+PPI
r11	FRU6P+GLN+ACoA+UTP→UDP-NAG+GLU+CoA+PPI
r12	UDPG+UDPNAG+2NAD+2ATP →HA+2UTP+2NADH+2ADP
r13	GLC6P+2NADP→R5P+NADPH+CO_2
r14	3R5P→2FRU6P+DHAP
r15	A+R5P+4ATP→ATPN+4ADP+PPI
r16	G+R5P+4ATP→GTP+4ADP+PPI
r17	U+R5P+4ATP→UTP+4ADP+PPI
r18	ATPN+NADPH→DATP+NADP
r19	GTP+NADPH→DGTP+NADP
r20	UTP+MTHF+2ATP+NADPH →DTTP+DHF+2ADP+NADP+PPI
r21	UTP+GLN+ATP→CTP+GLU+ADP+PI
r22	CTP+NADPH→DCTP+NADP
r23	100Amino acids +430.6ATP →100PROT+430.6ADP+430.6PI
r24	UDPG+3DHAP+3NADH+5ATP →TEIC+3NAD+5ADP+UTP+2PPI
r25	2UDPNAG+PEP+3.5ALA+GLU+LYS+8ATP+NADPH →PEPG+2UTP+8ADP+7PI+NADP
r26	UDPNAG+2GLC6P+2NADPH+3ATP →AWALL+UTP+2NADP+3ADP+2PPI
r27	23.9ACoA+2.1DHAP+0.65UDPG+43.5NADPH+ 24.3ATP +2.1NADH →LIP+23.9CoA+43.5NADP+24.3ADP+2.1NAD+ 0.65UTP+1.1PPI+2.2PI+2.1H_2O
r28	26.2ATPN+21.6UTP+32.2GTP+20CTP+40ATP →100RNA+40ADP+40PI+100PPI
r29	29DATP+29DTTP+21DGTP+21DCTP+137.2ATP →100DNA+137.2ADP+137.2PI+100PPI
r30	86.7PROT+2PEPG+1.6TEIC+0.7AWALL+1.1DNA +7.6RNA+0.5LIP →100BIOM
r31	2NADH+O_2→2NAD+H_2O
r32	ATP→ADP+PI

the exponential phase, there was a rapid increase in the biomass, HA, and by-product concentrations. Extra feed glucose was added late in the exponential phase to avoid the depletion of glucose and to maintain the concentration at 10 g/l. As the cells entered the stationary phase, the glucose catabolism decreased significantly and the HA concentration

remained unchanged as a result of the loss of HA synthesis capacity [5].

The main by-product was lactate, with a value of about 50 g/l at the end of the fermentation. In contrast, the acetate and ethanol concentrations were about 2 g/l and 1 g/l, respectively. It should be noted that no formate was detected during the HA fermentation, possibly due to the deactivation of pyruvate formate lyase (PFL) under aerobic conditions [22].

Metabolic Flux Distributions at Various DO Levels

The experiments were carried out at various DO levels, which were controlled by mixing air with oxygen or nitrogen. The impeller speed control was similar at the various DO levels. Moreover, an MFA was used to further explain the effect of the DO level on the HA molecular weight during HA fermentation.

This study used a modified metabolic flux model according to Fong Chong and Nielsen [8]. As PFL is inactive in the presence of oxygen [22], the model did not consider this reaction. The model consisted of the Embden-Meyerhof-Parnas (EMP) pathway, pentose phosphate pathway (PP), the reactions responsible for the fermentation products, and cofactor balances for ATP and NADH. The metabolic network of *S. zooepidemicus* is shown in Fig. 2.

The metabolic model consisted of 32 reactions, 6 measured metabolites, and 27 intracellular metabolites. The overdetermined system was solved by the least squares method [8]. The metabolic reactions of *S. zooepidemicus* are listed in Appendix I.

Based on the glucose uptake rate, HA and other by-product formation rate, and biomass formation rate, the cellular metabolic fluxes were calculated using a stoichiometric model. The metabolic flux distributions at various DO levels during the exponential phase are illustrated in Fig. 3, and normalized with respect to the glucose uptake rate.

S. zooepidemicus, a lactic acid bacterium, is often grown on complex media that are rich in amino acids (*e.g.*, yeast or peptone), providing the carbon skeletons for biosynthesis. However, the synthesis of biomass components only accounts for 5% of the carbon metabolized [8]. In

Appendix II. Abbreviations for the metabolites.

Measured metabolites	Intracellular metabolites	Others
Acetate (ACE)	Acetyl-CoA (ACoA)	Adenine (A)
Biomass (BIOM)	ATP	Adenosine diphosphate (ADP)
Ethanol (ETOH)	ATP incorporated into biomass (ATPN)	Alanine (ALA)
Glucose (GLC)	Antigenic wall polysaccharide (AWALL)	Carbon dioxide (CO_2)
Hyaluronic acid (HA)	Cytidine triphosphate (CTP)	Coenzyme A (CoA)
Lactate (LAC)	Deoxyadenosine triphosphate (DATP)	Dihydrofolate (DHF)
	Deoxycytidine triphosphate (DCTP)	Guanine (G)
	Deoxyguanosine triphosphate (DGTP)	Glutamine (GLN)
	Deoxythymidine triphosphate (DTTP)	Glutamate (GLU)
	Dihydroxyacetone phosphate (DHAP)	Glycine (GLY)
	Deoxyribonucleic acid (DNA)	Water (H_2O)
	Fructose-6-phosphate (FRU6P)	Lysine (LYS)
	Glucose-6-phosphate (GLC6P)	N^5, N^{10}-methylene-THF (MTHF)
	Guanosine triphosphate (GTP)	Nicotinamide adenine dinucleotide (oxidized) (NAD)
	Lipid (LIP)	NAD phosphate (oxidized) (NADP)
	Nicotinamide adenine dinucleotide (reduced) (NADH)	Oxygen (O_2)
	NAD phosphate (reduced) (NADPH)	Orthophosphate (PI)
	Phosphoenolpyruvate (PEP)	Pyrophosphate (PPI)
	Peptidoglycan (PEPG)	Uracil (U)
	Protein (PROT)	
	Pyruvate (PYR)	
	Ribose-5-phosphate (R5P)	
	Ribonucleic acid (RNA)	
	Teichoic acid (TEIC)	
	UDP-glucose (UDPG)	
	UDP-*N*-acetylglucosamine (UDPNAG)	
	Uridine triphosphate (UTP)	

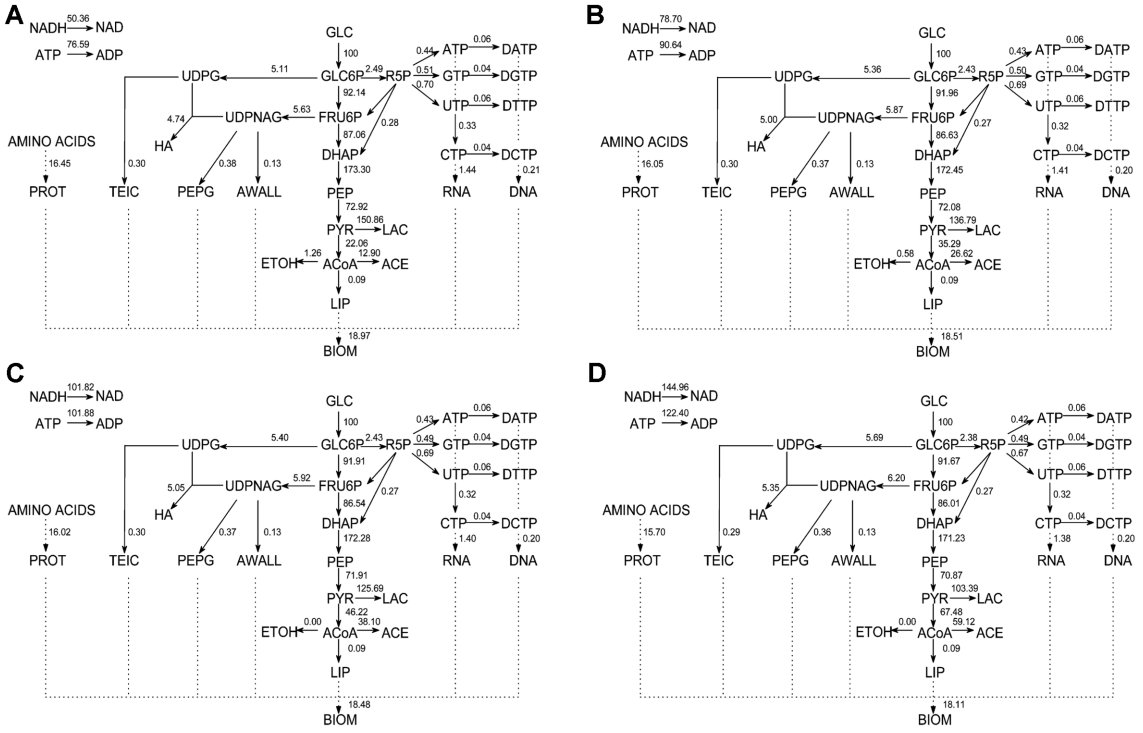

Fig. 3. Flux distribution for the exponential phase of HA fermentation at different DO levels.
A. 10%; **B**. 30%; **C**. 50%; **D**. 80%. The flux estimates are normalized with respect to the specific glucose uptake.

Fig. 3, there was no significant difference in the biomass concentration.

Lactate, acetate, and ethanol were the by-products during the HA fermentation, and substantial changes in the flux distribution through their pathways were observed at various DO levels. The flux of lactate decreased with the DO level, as the lactate dehydrogenase (LDH) was attenuated by the lower ratio of NADH/ NAD^+ [8, 25]. In contrast, the flux of acetate exhibited an increase, which was attributed to enhanced pyruvate dehydrogenase (PDH) activity due to the lower ratio of NADH/ NAD^+ [9]. It should be noted that no ethanol was detected at DO levels of 50% and 80%, possibly due to the low activity of the alcohol dehydrogenase enzyme under aeration [24].

However, the flux through the HA synthesis pathway was little affected at the various DO levels. The network of GLC6P and FRU6P, which is considered a dependent network, contribute a stoichiometrically consumed component of HA [26]. Yet, the flux partitionings at both the GLC6P node and FRU6P code were unchanged at the various DO levels, and the majority of the trunk flux (r_1) was through the EMP pathway (more than 90%). In contrast, the flux of the HA synthesis pathway was approximately 5%, demonstrating a dependent network of HA synthesis that harbors two rigid nodes. Previously, Fong Chong and Nielsen [8] found that the flux partitioning at both the GLC6P node and FRU6P code was unaffected by a change in the carbon source, yet resulted in a 40% attenuation of all metabolic fluxes in maltose when compared with glucose. Therefore, it would seem that the flux of the HA synthesis pathway is not easily changed by environment perturbation, owing to the rigid network of HA synthesis.

Effect of ATP Production on HA Molecular Weight

Oxygen can be used by *S. zooepidemicus* to oxidize NADH into NADH oxidase (NOX), due to the absence of oxidative phosphorylation [7]. Thus, the expression of NOX increased under aeration conditions, and shifted the flow between LDH and PDH [8, 9]. Therefore, more ATP was concomitantly generated with the excretion of acetate.

Table 1 shows the ATP production during HA fermentation at the various DO levels. ATP was generated by substrate-level phosphorylation, and the amount calculated based on $r_4+r_5+r_{10}-r_3$. It was found that the ATP production was enhanced with a high level of DO, which was attributed to high acetate formation. HA has a high molecular mass, usually in the order of millions of daltons. Thus, the synthesis of 1 mol unit of HA disaccharide consumes 2 mol glucose,

Table 1. The production of ATP at various DO levels.

DO (%)	r_{ATP} (mmol/g biomass/h)
10	54.0±2.5
30	56.5±2.8
50	61.3±2.4
80	68.4±2.0

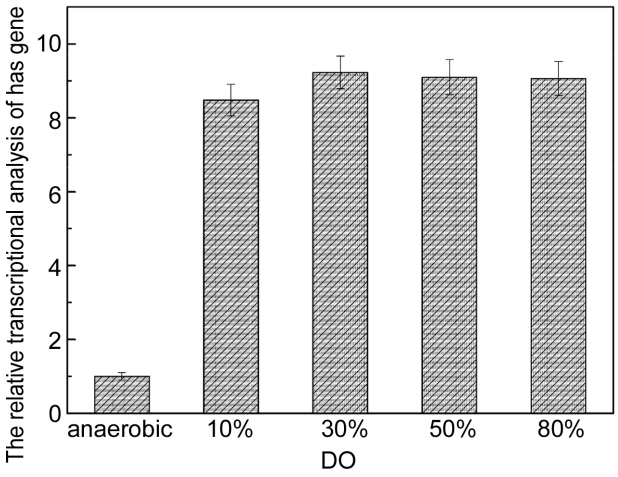

Fig. 4. Effect of DO level on the expression of the *has* gene during HA fermentation of *S. zooepidemicus* G1.
has gene expression under anaerobic condition was designated as control.

5 mol ATP equivalents, and 1 mol acetyl-coenzyme A [28]. Therefore, the higher HA molecular weight with a high level of DO may have been related to the additional generation of ATP due to the higher acetate formation at a high DO level.

has Gene Expression and HAS Activity

The HAS enzymes, which are the key enzymes in HA biosynthesis, process at least six distinct functions, including two sugar nucleotide-binding sites, two different glycosyltransferase activities, one or more binding sites for elongating the HA-UDP chain, and the ability to transfer the HA chain [27]. In this study, the *has* gene expression and HAS activity were determined under both anaerobic and aerobic conditions, and the transcription levels of the *has* gene are compared in Fig. 4. The expression of the *has* gene was completely repressed under anaerobic conditions, resulting in a 9-fold higher expression of the *has* gene under aerobic conditions compared with that under anaerobic conditions. Notwithstanding, there was no significant difference in the expression of the *has* gene at the various DO levels.

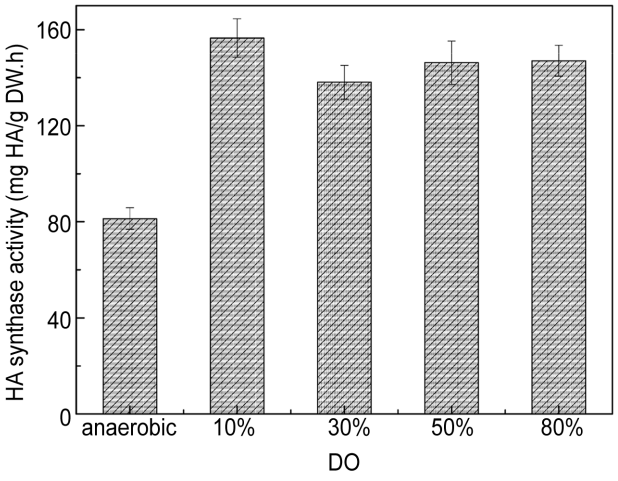

Fig. 5. Effect of DO level on HAS activity during HA fermentation of *S. zooepidemicus* G1.

Table 2. HA yield and molecular weight at various DO levels [6].

DO level (%)	HA yield HA (g/l)	HA molecular weight ($\times 10^6$ Da)
Anaerobic	0.73±0.04	1.22±0.02
10	3.55±0.08	1.75±0.06
30	3.48±0.09	1.90±0.04
50	3.51±0.08	2.19±0.05
80	3.50±0.10	2.06±0.02

The HAS activity results under both anaerobic and aerobic conditions are summarized in Fig. 5. Under anaerobic conditions, the HAS activity was about 80 mg HA/g DW-h, whereas under aerobic conditions, the HAS activity was almost 2-fold higher; however, there was no significant difference in the HAS activity at the various DO levels. It should be noted that the effect of the DO level on the HAS activity was consistent with its effect on the HA yield, as reported previously (Table 2). Therefore, the *has* gene expression and HAS activity results may explain the reason why the HA production was repressed under anaerobic conditions.

Effect of Reactive Oxygen Species on HA Molecular Weight

It has already been observed that the HA molecular weight increases with an increasing DO level, yet decreases with a DO level of 80% [6]. Meanwhile, *in vitro* studies have shown that HA is degraded by ROS damage, and this degradation accelerates when increasing the concentration of ROS [23, 24]. Therefore, it is proposed that the generation of ATP and ROS has a concomitant effect on the HA molecular weight, and the balance of this effect then causes the variation in the HA molecular weight at various DO levels. The production of ROS, including hydrogen peroxide (H_2O_2), superoxide ($O_2^{-}\cdot$), and hydroxyl radicals (OH·), increased proportionally with the partial oxygen pressure [4, 14]. Fig. 6 shows the relative ROS levels in *S. zooepidemicus* under both anaerobic and aerobic conditions. The generation of ROS increased with an increase in the DO level, and reached a maximum during the mid-exponential growth phase. Hence, the decrease in the HA molecular weight may have been due to the effect of ROS generation during the HA fermentation at a high DO level.

Thus, the inference is that the HA molecular weight would seem to depend on the generation of ATP and ROS. The generation of ATP also increased proportionally with the DO level, similar to the generation of ROS. At a low DO level, the ATP generation seemed to play a more major role in the HA synthesis than the ROS. However, when the

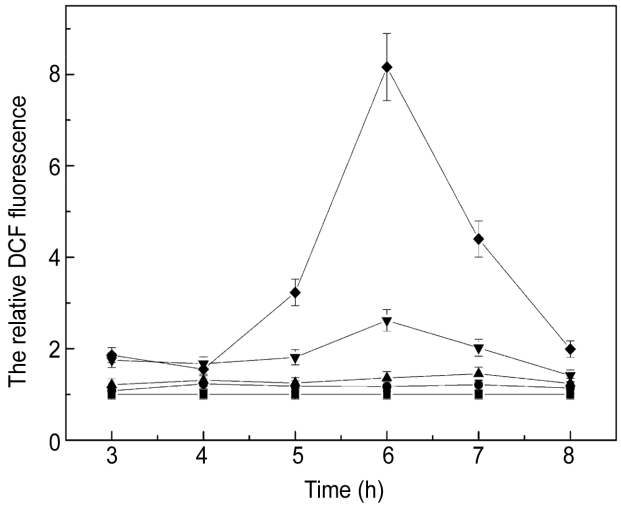

Fig. 6. Effect of DO levels on the generation of ROS during HA fermentation of *S. zooepidemicus* G1.
Symbols: (■), anaerobic condition; (●), 10% DO; (▲), 30% DO; (▼), 50% DO; (◆), 80% DO. The anaerobic condition was designated as control.

generation of ROS increased with a high DO level, there was a decrease in the HA molecular weight. Therefore, an appropriate DO level favored the HA molecular weight.

In summary, the metabolic flux distributions of *S. zooepidemicus* at various DO levels were compared to illustrate the effect of the DO level on the HA yield and molecular weight. The flux through the HA synthesis pathway was little affected by the DO level, owing to the rigid network of HA synthesis; however, more ATP was produced concomitant with acetate when increasing the DO level. Meanwhile, the *has* gene expression and HAS activity were both found to be inhibited under anaerobic conditions, yet minimally influenced by the DO level under aerobic conditions. In addition, excessive ROS was generated at a high DO level. Thus, in terms of the mechanism of the effect of oxygen on the HA molecular weight, it was concluded that, since ATP favors the HA molecular weight, whereas ROS degrades the HA molecular weight, the concomitant effect of the generation of ATP and ROS determines the HA molecular weight. Therefore, a proper DO level for HA production by *S. zooepidemicus* needs to be maintained to obtain the optimum HA molecular weight.

REFERENCES

1. Armstrong, D. C. and M. R. Johns. 1997. Culture conditions affect the molecular weight properties of hyaluronic acid produced by *Streptococcus zooepidemicus*. *Appl. Environ. Microbiol.* **63:** 2759–2764.
2. Bai, D. M., X. M. Zhao, X. G. Li, and S. M. Xu. 2004. Strain improvement of *Rhizopus oryzae* for over-production of $_{L}$(+)-lactic acid and metabolic flux analysis of mutants. *Biochem. Eng. J.* **18:** 41–48.
3. Bitter, T. and H. M. Muir. 1962. A modified uronic acid carbazole reaction. *Anal. Biochem.* **4:** 330–333.
4. Bunn, H. F. and R. O. Poyton. 1996. Oxygen sensing and molecular adaptation to hypoxia. *Physiol. Rev.* **76:** 839–885.
5. Crater, D. L. and I. van de Rijn. 1995. Hyaluronic acid synthesis operon (*has*) expression in group A Streptococci. *J. Biol. Chem.* **270:** 18452–18458.
6. Duan, X.-J., L. Yang, X. Zhang, and W.-S. Tan. 2008. Effect of oxygen and shear stress on molecular weight of hyaluronic acid produced by *Streptococcus zooepidemicus*. *J. Microbiol. Biotechnol.* **18:** 718–724
7. Fong Chong, B., L. M. Blank, R. McLaughlin, and L. K. Nielsen. 2005. Microbial hyaluronic acid production. *Appl. Microbiol. Biotechnol.* **66:** 341–351.
8. Fong Chong, B. and L. K. Nielsen. 2003. Aerobic cultivation of *Streptococcus zooepidemicus* and the role of NADH oxidase. *Biochem. Eng. J.* **16:** 153–162.
9. Fong Chong, B. and L. K. Nielsen. 2003. Amplifying the cellular reduction potential of *Streptococcus zooepidemicus*. *J. Biotechnol.* **100:** 33–41.
10. Gao, H. J., G. C. Du, and J. Chen. 2006. Analysis of metabolic fluxes for hyaluronic acid (HA) production by *Streptococcus zooepidemicus*. *World J. Microbiol. Biotechnol.* **22:** 399–408.
11. Hasegawa, S., M. Nagatsuru, M. Shibutani, S. Yamamoto, and S. Hasebe. 1999. Productivity of concentrated hyaluronic acid using a maxblend fermentor. *J. Biosci. Bioeng.* **88:** 68–71.
12. Huang, W-C., S.-J. Chen, and T.-L. Chen. 2006. The role of dissolved oxygen and function of agitation in hyaluronic acid fermentation. *Biochem. Eng. J.* **32:** 239–243.
13. Kang, S.-W., E. R. Cho, and B.-S. Kim. 2005. PLGA microspheres in hyaluronic acid gel as a potential bulking agent for urologic and dermatologic injection therapies. *J. Microbiol. Biotechnol.* **15:** 510–518.
14. Kietzmann, T., J. Fandrey, and H. Acker. 2000. Oxygen radicals as messengers in oxygen-dependent gene expression. *News Physiol. Sci.* **15:** 202–208.
15. Kim, J.-H., S.-J. Yoo, D.-K. Oh, Y.-G. Kweon, D.-W. Park, C.-H. Lee, and G.-H. Gil. 1996. Selection of a *Streptococcus* equimutant and optimization of culture conditions for the production of molecular weight hyaluronic acid. *Enzyme Microb. Technol.* **19:** 440–445.
16. Kim, S.-J., S.-Y. Park, and C.-W. Kim. 2006. A novel approach to the production of hyaluronic by *Streptococcus zooepidemicus*. *J. Microbiol. Biotechnol.* **16:** 1849–1855.
17. Kim, T. Y. and S. Y. Lee. 2006. Accurate metabolic flux analysis through data reconciliation of isotope balance-based data. *J. Microbiol. Biotechnol.* **16:** 1139–1143.
18. Kogan, G., L. Šoltés, R. Stern, and P. Gemeiner. 2007. Hyaluronic acid: A natural biopolymer with a broad range of biomedical and industrial applications. *Biotechnol. Lett.* **29:** 17–25.
19. Laurent, T. C., M. Ryan, and A. Pietruszkiewicz. 1960. Fraction of hyaluronic acid. The polydispersity of hyaluronic acid from the bovine vitreous body. *Biochim. Biophys. Acta* **42:** 476–485.
20. Liu, H. J., Q. Li, D. H. Liu, and J. J. Zhong. 2006. Impact of hyperosmotic condition on cell physiology and metabolic flux distribution of *Candida krusei*. *Biochem. Eng. J.* **28:** 92–98.
21. Miller, G. L. 1959. Use of dinitrosalicylic reagent for determination of reducing sugars. *Anal. Chem.* **31:** 426–428.

22. Nordkvist, M., N. B. Siemsen Jensen, and J. Villadsen. 2003. Glucose metabolism in *Lactococcus lactis* MG1363 under different aeration conditions: Requirement of acetate to sustain growth under microaerobic conditions. *Appl. Environ. Microbiol.* **69:** 3462–3468.
23. Praest, B. M., H. Greiling, and R. Kock. 1997. Effects of oxygen-derived free radicals on the molecular weight and the polydispersity of hyaluronan solutions. *Carbohydr. Res.* **303:** 153–157.
24. Presti, D. and J. E. Scott. 1994. Hyaluronan-mediated protective effect against cell damage caused by enzymatically produced hydroxyl (OH·) radicals is dependent on hyaluronan molecular mass. *Cell Biochem. Funct.* **12:** 281–288.
25. Siemsen Jensen, N. B., C. R. Melchiorsen, K. V. Jokumsen, and J. Villadsen. 2001. Metabolic behavior of *Lactococcus lactis* MG1363 in microaerobic continuous cultivation at a low dilution rate. *Appl. Environ. Microbiol.* **67:** 2677–2682.
26. Stephanopoulos, G. and J. J. Vallino. 1991. Network rigidity and metabolic engineering in metabolite overproduction. *Science* **252:** 1675–1681.
27. Tlapak-Simmons, V. L., B. A. Baggenstoss, K. Kumari, C. Heldermon, and P. H. Weigel. 1999. Kinetic characterization of the recombinant hyaluronan synthases from *Streptococcus pyogenes* and *Streptococcus equisimilis*. *J. Biol. Chem.* **274:** 4246–4253.
28. Widner, B., R. Behr, S. Von Dollen, M. Tang, T. Heu, A. Sloma, *et al*. 2005. Hyaluronic acid production in *Bacillus subtilis*. *Appl. Environ. Microbiol.* **71:** 3747–3752.
29. Yu, H. and G. Stephanopoulos. 2008. Metabolic engineering of *Escherichia coli* for biosynthesis of hyaluronic acid. *Metab. Eng.* **10:** 24–32.